THE JOURNAL OF PHYSICAL CHEMISTRY A

Article

pubs.acs.org/JPCA

Quantum Dynamics of Vinylidene Photodetachment on an Accurate Global Acetylene-Vinylidene Potential Energy Surface

Lifen Guo,[†] Huixian Han,[‡,§] Jianyi Ma,*[,†] and Hua Guo*[,‡]

[†]Institute of Atomic and Molecular Physics, Sichuan University, Chengdu, Sichuan 610065, China

[‡]Department of Chemistry and Chemical Biology, University of New Mexico, Albuquerque, New Mexico 87131, United States

[§]School of Physics, Northwest University, Xi'an, Shaanxi 710069, China

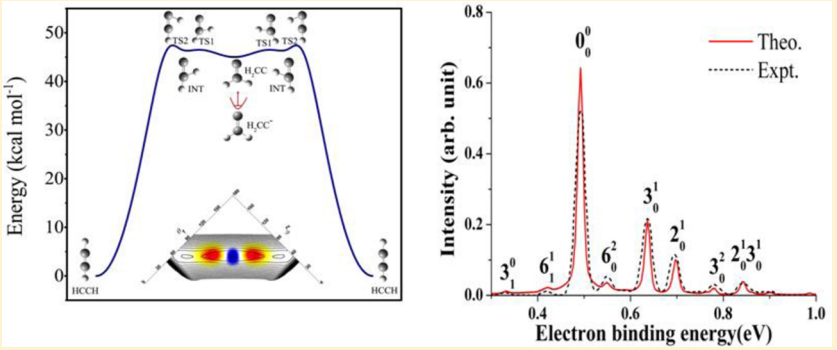

ABSTRACT: Vinylidene is a high-energy isomer of acetylene, and the rearrangement of bonds in the two species serves as a prototype for isomerization reactions. Here, a full-dimensional quantum mechanical study of the vinylidene vibration is carried out on a recently developed global acetylene−vinylidene potential energy surface by simulating the photodetachment dynamics of the vinylidene anion. Several low-lying vibrational levels of the anion were first determined on a new ab initio based potential energy surface, and their photoelectron spectra were obtained within the Condon approximation. The vibrational features of the vinylidene isomer are found to agree well with the experiment in both positions and intensities, validating the global acetylene−vinylidene potential energy surface.

I. INTRODUCTION

Vinylidene (H_2CC), a high-energy isomer of acetylene (HCCH), is known to play an important role in many reactive environments, including combustion.[1] As a prototype for the 1,2-hydrogen shift,[2] the isomerization dynamics between the two isomers has attracted much attention in the past.[3−6] Experimentally, the large amplitude bending vibrations of acetylene along the isomerization pathway have been probed spectroscopically by Field and co-workers.[7−12] Highly excited bending overtones on the ground electronic state have been identified via stimulated emission and fluorescence techniques to energies just below the isomerization barrier, although direct spectroscopic detection of vinylidene has so far been unsuccessful.[13] These spectroscopic studies have revealed interesting patterns in the form of a normal-to-local transition for the acetylene bending vibrations.[5,14] The isomerization dynamics has also been investigated experimentally by Lineberger and co-workers using negative ion photodetachment.[15,16] The ejection of an electron from the stable vinylidene anion places the system on the neutral state near the vinylidene isomer, and the ensuing dynamics manifests in the form of vibrational features in the photoelectron spectrum. Spectral widths of these features were estimated from the spectrum, which seem to imply relatively short "lifetimes" (a few picoseconds) for the vinylidene features. However, a subsequent Coulomb explosion experiment suggested a very "long-lived" vinylidene.[17] It should be noted that these seemingly different conclusions deduced from the above experiments are somewhat dubious, as the lifetime of the bound vinylidene isomer is, rigorously speaking, infinity.

Parallel to the extensive experimental work, many theoretical studies on both the spectroscopic and dynamical aspects of the acetylene−vinylidene isomerization process have been reported. Detailed investigations using effective Hamiltonians[18−28] as well as full-dimensional quantum mechanical methods[29−32] have successfully reproduced the normal-to-local transition in the acetylene bending manifold without the explicit consideration of vinylidene. Both reduced and full-dimensional models for the isomerization dynamics have also been proposed,[33−39] which require an accurate description of the global potential energy surface (PES). Many of the earlier studies relied on approximate PESs,[40−42] but the situation has significantly improved recently.[43−47] It is well-established from high-level ab initio calculations that vinylidene is characterized by a potential minimum bound only by a small dissociation barrier. In particular, Zou and Bowman (ZB) in 2003 reported

Received: May 27, 2015
Revised: June 19, 2015
Published: June 24, 2015

DOI: 10.1021/acs.jpca.5b05061
J. Phys. Chem. A 2015, 119, 8488−8496

a global full-dimensional PES based on high-level ab initio calculations.[48] Several full-dimensional quantum mechanical calculations on the ZB PES have since been published for both acetylene[49,50] and vinylidene.[49−56] While providing a valuable perspective on the landscape of the isomerization pathway, however, the ZB PES is not spectroscopically accurate, and quantum dynamical calculations of the acetylene spectrum have uncovered substantial differences from experimental band origins.[57] Very recently, we reported a new and much more accurate global PES fitted to a large number of high-level ab initio points over a large configuration space covering both isomers.[58] The high fidelity of the fitting was achieved by the recently proposed permutation invariant polynomial-neural network (PIP-NN) method, which is based on a permutation symmetry-adapted neural network scheme.[59,60] Full-dimensional quantum dynamical calculations in the acetylene well on this PIP-NN PES reproduced experimental band origins up to 13000 cm^{-1} with near-spectroscopic accuracy.[58] However, the validity of the PES in the vinylidene region has not been rigorously tested. To that end, we report here an accurate semiglobal PES for the vinylidene anion and a full-dimensional quantum dynamical investigation of its photodetachment. The latter goes beyond the Franck−Condon model and provides useful information on mode-specific "lifetimes" of the vinylidene vibrational features in the limit of an infinite density of states. We emphasize here that all states below the dissociation limit are discrete so the use of this limit in simulating the spectrum is purely for convenience. The thermally averaged photoelectron spectrum is found to reproduce the experiment very well in both position and intensity, suggesting convincingly that the PIP-NN PES provides a quantitatively accurate description of the vinylidene vibration and isomerization, in addition to the acetylene vibration. The availability of a globally accurate PES is expected to stimulate further dynamical studies of the prototypical isomerization process.

II. POTENTIAL ENERGY SURFACES

The neutral acetylene−vinylidene PES reported in our earlier work[58] was based on a PIP-NN fit of 37000 ab initio points at the explicitly correlated couple-cluster singles, doubles, and perturbative triples (CCSD(T)-F12a) level[61,62] with the correlation-consistent triple-ζ basis set optimized for describing core−valence correlation effects (cc-pCVTZ-F12).[63,64] It is a global PES covering both the HCCH and H_2CC regions with a root-mean-square error (RMSE) less than 10 cm^{-1}. In Figure 1, the minimum energy path (MEP) for the isomerization between acetylene and vinylidene is shown. An important feature of the MEP is the existence of a metastable intermediate (INT), in addition to the C_{2v} vinylidene isomer. In addition, it was shown that, although the isomerization is dominated by large amplitude motion of the two hydrogen atoms, the C−H bonds undergo significant changes.[58] As a result, a purely large amplitude bending model is insufficient to describe the isomerization process. Instead, a full-dimensional quantum model is needed.

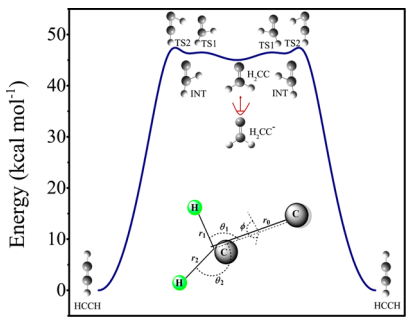

Figure 1. Minimum energy path for the isomerization between acetylene to vinylidene. Inset: The Radau-Jacobi coordinates used to describe the H_2CC systems.

In order to determine the proper ab initio method for mapping out the anion PES, the equilibrium structure and harmonic frequencies of the H_2CC^- system were first calculated. The explicitly correlated version of the spin-unrestricted CCSD(T) (UCCSD(T)-F12a) method[61,62] was used, with both the frozen-core (FC) and all-electron (AE) treatments. Peterson's cc-pCVXZ-F12(X=T,Q) basis sets[63,64] were tested. These methods are denoted as FC-UCCSD(T)/cc-pCVXZ-F12(X=T,Q) and AE-UCCSD(T)/cc-pCVXZ-F12-(X=T,Q), respectively. The calculated equilibrium geometry, zero point energy, and harmonic vibrational frequencies of H_2CC^- are compared with previous theoretical results[45] and available experimental data[16,65] in Table 1. (For comparison, the equilibrium geometry and vibrational frequencies of the neutral vinylidene are also included in the table.) It can be seen from Table 1 that all our calculated equilibrium parameters are in good agreement with experimental values, and the core electron correlation has a relatively small effect on harmonic frequencies for this system. Comparing the results of FC-UCCSD(T)/cc-pCVTZ-F12 and AE-UCCSD(T)/cc-pCVQZ-F12, the differences in the harmonic vibrational frequencies are 5.60, 4.76, 5,73, 3,72, 1.64, and 7.64 cm^{-1} for the CH symmetry stretching (ν_1), CH asymmetry stretching (ν_5), CC stretching (ν_2), CH_2 scissors (ν_3), CH_2 rock (ν_6), and out-of-plane (ν_5) modes, respectively. (In Figure 2, the normal mode vectors of these vibrational modes, which are applicable for both neutral and anionic vinylidene, are depicted.) We thus conclude that the accuracy of the FC-UCCSD(T)/cc-pCVTZ-F12 method is sufficient for studying the photodetachment spectra of this system. The ab initio points were chosen in the region $R_{CC}\in[1.0, 1.45]$ Å, $R_{CH}\in[0.9, 1.50]$ Å, $\theta_{HCC}\in[50°, 180°]$; and $\varphi\in[0°, 180°]$ points were chosen on a (uneven) grid, and those above the energy cutoff were discarded. All ab initio calculations were carried out using the MOLPRO suite of electronic structure programs.[66]

A total of 9830 points with energies below the cutoff of 2.25 eV (18147 cm^{-1}) from the potential minimum were selected to construct the PES. This semiglobal H_2CC^- PES was fitted using the PIP-NN approach[59,60] similar to our previous work on the neutral acetylene−vinylidene system.[58] All 75 PIPs[67] up to the fourth order were used as the symmetry functions in the input layer of the NN. The NN fittings were performed using the Levenberg−Marquardt algorithm with the RMSE as the performance function:

$$\mathrm{RMSE} = \sqrt{\frac{1}{n}\sum_{i=1}^{n}(E_{\mathrm{fit}} - E_{\mathrm{calc}})^2} \quad (1)$$

III. QUANTUM DYNAMICS

The full-dimensional quantum dynamical calculation of the photodetachment of the vinylidene anion was performed using the (2 + 1) Radau-Jacobi coordinates,[68] denoted as $(r_0,r_1,r_2,\theta_1,\theta_2,\phi)$. As shown in the inset in Figure 1, r_0 is distance between C and the center of mass of CH_2, r_1 and r_2 are

DOI: 10.1021/acs.jpca.5b05061
J. Phys. Chem. A 2015, 119, 8488−8496

Table 1. Optimized Equilibrium Geometries (Å and Degree), Zero Point Energy (ZPE, cm^{-1}), and Harmonic Frequencies (cm^{-1}) for the H_2CC^- System in Comparison with Available Experimental and Theoretical Data[a]

	r_{CC}	r_{CH}	θ_{HCC}	ZPE	(ν_1) CH sym. str.	(ν_5) CH asym. str.	(ν_2) CC str.	(ν_3) CH_2 scissor	(ν_6) CH_2 rock	(ν_4) out-of-plane
FC-UCCSD(T)-F12a/cc-pCVTZ-F12	1.3438	1.1056	123.52	5091.1	2865.9	2837.8	1502.0	1335.2	876.5	764.9
FC-UCCSD(T)-F12a/cc-pCVQZ-F12	1.3435	1.1054	123.52	5091.7	2865.2	2837.0	1501.6	1334.9	876.2	768.5
AE-UCCSD(T)-F12a/cc-pCVTZ-F12	1.3403	1.1040	123.51	5105.3	2872.3	2843.4	1507.8	1339.7	878.5	768.9
AE-UCCSD(T)-F12a/cc-pCVQZ-F12	1.3400	1.1039	123.51	5105.8	2871.5	2842.5	1507.7	1339.2	878.1	772.6
Theory[b]	1.3668	1.1187	123.53		2865	2844	1497	1326	869	772
Anharmonic[b]					2267	2621	1462	1289	846	748
PIP-NN PES	1.3437	1.1056	123.52	5100.5	2869.8	2840.1	1504.5	1335.3	875.3	776.3
QM				4998.3	2668.1	2618.1	1460.2	1297.2	853.6	759.4
Experiment	1.347 ± 0.007[c]	1.119 ± 0.006[c]	124.0 ± 0.2[c]		2663 ± 5[d]	2606 ± 5[d]	1485 ± 30[c]	1305 ± 10[c]	–	–
H_2CC (PIP-NN)[e]	1.3000	1.0865	120.1	5150.9	3121.8	3223.1	1682.9	1221.3	327.6	725.2

[a]The equilibrium geometry and harmonic frequencies of the neutral vinylidene are also included for comparison. [b]FC-UCCSD(T)/aug-cc-pVDZ.[45] [c]Fundamental frequencies.[16] [d]Fundamental frequencies.[65] [e]Ref 58.

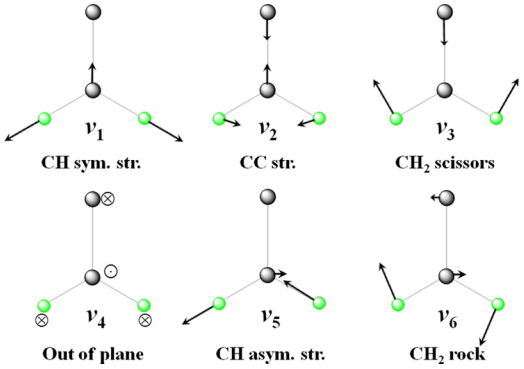

Figure 2. Normal mode vectors for vinylidene vibrations in both neutral and anionic forms.

two Radau radial coordinates for the CH_2 species, θ_1 (θ_2) is the angle between vectors $\vec{r}_1$ ($\vec{r}_2$) and $\vec{r}_0$, and ϕ is the relative azimuthal angle between $\vec{r}_1$ and $\vec{r}_2$ in the body-fixed (BF) frame, which has the z axis along $\vec{r}_0$. The rotationless (J = 0) Hamiltonian in the (2 + 1) Radau-Jacobi coordinate system is given as follows ($\hbar$ = 1):

$$\hat{H} = -\frac{1}{2\mu_0}\frac{\partial^2}{\partial r_0^2} + \sum_{i=1}^{2}\left(-\frac{1}{2\mu_i}\frac{\partial^2}{\partial r_i^2}\right) + \sum_{i=0}^{2}\frac{\hat{j}_i^2}{2\mu_i r_i^2} + V(r_0, r_1, r_2, \theta_1, \theta_2, \phi) \quad (2)$$

where $\mu_0 = m_C(m_C + 2m_H)/(2m_H + 2m_C)$, $\mu_1 = \mu_2 = m_H$. $\hat{j}_1$ and $\hat{j}_2$ are the angular momentum operators for r_1 and r_2, respectively, and $\hat{j}_0^2 = (\hat{j}_1 + \hat{j}_2)^2$. V is the potential energy function defined in Radau-Jacobi coordinates. The Hamiltonian is discretized using a mixed grid-basis representation.[69] The radial coordinates r_1 and r_2 are represented by DVR (discrete variable representation)[70] grids, and r_0 is represented by PODVR (potential optimized DVR),[71,72] while the angular coordinates by basis functions.

Following our recent work,[73,74] the initial wave packets (Ψ_i) on the neutral PES were assumed, within the Condon approximation, to arise from a vertical transition from the anion PES. The anion wave functions for the four lowest-lying rotationless vibrational levels (J = 0) were obtained by diagonalizing the same Hamiltonian eq 2 using the anion PES described above with the Lanczos method.[75]

The wave packet on the neutral state PES is propagated using the real Chebyshev propagator:[76]

$$\Psi_k = 2D\hat{H}_s\Psi_{k-1} - D^2\Psi_{k-2},\ k \geq 2 \quad (3)$$

with $\Psi_1 = D\hat{H}_s\Psi_0$ and $\Psi_0 = \Psi_i$. The Hamiltonian in eq 3 was scaled to the spectral range of (−1,1) via $\hat{H}_s = (\hat{H} - H^+)/H^-$. The spectral medium [$H^+ = (H_{max} + H_{min})/2$] and half width [$H^- = (H_{max} - H_{min})/2$] were determined by the spectral extrema, H_{max} and H_{min}, which can be estimated easily. Finally, the wave packet was damped near the edge of the grids of the radial coordinates of r_1 and r_2, and the damping functions (D) and parameters are listed in Table 2.

Table 2. Numerical Parameters (in a.u.) Used in Wave Packet Calculations

system	H_2CC
grid/basis ranges and sizes	r_1,r_2 ∈ (1.5,5.0) $N_1 = N_2$ = 22 13 PODVR for r_0
largest values of j_1, j_2 and m	35, 35, 35
damping potential for r_1, r_2[a]	α_d = 0.1, r_i^d = 3.0
propagation steps	40000

[a]The damping function is defined as $D = \exp[-\alpha_d(r_i - r_i^d)^2]$, $r_i \geq r_i^d$

The photoelectron spectra were obtained from the discrete cosine Fourier transform of the Chebyshev autocorrelation functions $C_k \equiv \langle\Psi_0|\Psi_k\rangle$:[77]

$$S(E) = \frac{1}{\pi H^- \sin\vartheta}\sum_{k=0}(2 - \delta_{k,0})\cos(k\vartheta)C_k \quad (4)$$

DOI: 10.1021/acs.jpca.5b05061
J. Phys. Chem. A 2015, 119, 8488−8496

where $\vartheta = \arccos E_s$ is the Chebyshev angle, k is the Chebyshev order, and E_s is the scaled total energy corresponding to $\hat{H}_s$. For narrow resonances, we have also determined their complex energies $(E_n - i\Gamma_n/2)$ from the Chebyshev correlation functions using a low-storage filter diagonalization method.[75]

It should be noted that the damping scheme described above, which has been used by others,[34,37,54] makes an important assumption that the density of states outside the vinylidene region is infinity. In other words, a wave packet entering the acetylene region will not be allowed to come back to the vinylidene region. This is a strong assumption, which is only true in the short-time limit. As a result, the lifetimes determined using the current damping approach can only be compared with low-resolution spectra.

III. RESULTS AND DISCUSSION

In the PIP-NN fitting of the anion PES, the data were divided randomly into three sets, namely the training (90% of the data points), validation (5%), and test (5%) sets. After testing several two-layer NN structures with different numbers of interconnecting neurons, a two-layer NN with 35 and 35 neurons, NN(35−35), with 3921 parameters was employed. The RMSEs for the training, validation, testing sets, and maximum deviation of the final PESs are 1.61, 6.53, 69.37, and 308.91 cm^{-1}, respectively. The final RMSE is 10.56 cm^{-1}. The fitting errors for the final PES is shown in Figure 3 as a function

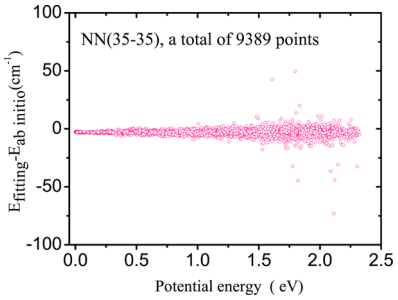

Figure 3. Fitting errors for the NN(35−35) anion PES as a function of their corresponding ab initio energies.

of the ab initio energy, and they are small and evenly distributed over the entire energy range. In Figure 4, contours of the anion PES near its equilibrium geometry are plotted. As shown, the PES is very smooth and well-behaved.

The fundamental vibrational frequencies of the H_2CC^- anion have been computed on the PIP-NN PES and are listed in the QM row of Table 1. Except for the frequency of the CH asymmetric stretching mode, which has an error of a few cm^{-1} with the experimental result, all of the theoretical frequencies are within the experimental error bounds. Also note that our frequencies are generally in better agreement with the experiment than those reported earlier by Stanton et al.,[45] particularly for the stretching modes, validating the accuracy of the PES.

In Figure 5, the calculated thermal averaged photoelectron spectrum of the vinylidene anion is compared with the experimental result of Ervin et al.[16] Since the experiment was performed at 450 K,[16] several low-lying vibrational states (0_0, 4_1, 6_1, 3_1) of the anion were included in the calculation of the spectrum and their contributions were weighted by the Boltzmann factors. In addition, the theoretical spectrum is convoluted by a Gaussian with the width of 5 meV in order to

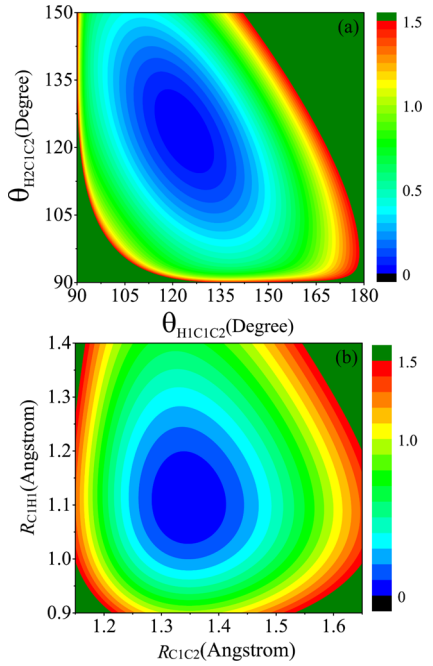

Figure 4. Contours of the PIP-NN anion PES, (a) as a function of θ_{H1C1C2} and θ_{H2C1C2}, with all other internal coordinates optimized and (b) along R_{C1C2} and R_{C1H1} with all other internal coordinates optimized.

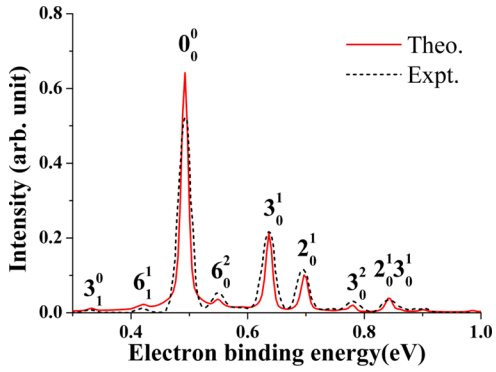

Figure 5. Calculated (red line) and experimental (black line) photoelectron spectra of H_2CC^- at 450 K. The theoretical result is convoluted with a Gaussian function (σ = 5 meV) and the experimental line corresponds to the convoluted Franck−Condon simulation reported in ref 16.

compare with the low-resolution experiment. It is clear that the theoretical result matches the experiment spectrum very well in both peak positions and intensities, including the hot bands.

In the experiment of Lineberger and co-workers,[16] the assignments of the vinylidene peaks were determined using scaled ab initio frequencies at the Hartree−Fock level. No such scaling is necessary here as our vibrational frequencies of vinylidene are accurate, as shown in Table 3. Our results confirm the assignments of the main peaks in the experimental photoelectron spectrum. For some of weak peaks at higher energies, the corresponding wave functions are mixed with CH_2 scissors, CC stretching, and CH_2 rock features.

To better understand the photodetachment process, we plotted in Figure 6 the unconvoluted theoretical photoelectron spectra for several low-lying vibrational states of the H_2CC^- anion, and the corresponding energy levels and the lifetimes of

DOI: 10.1021/acs.jpca.5b05061
J. Phys. Chem. A 2015, 119, 8488−8496

Table 3. Energies and Lifetimes (τ) of Vinylidene (H_2CC) States

	theo. (present work)			theo.[55]		theo.[56]	
assign.	energy	τ (ps)	$\nu^n - \nu^{n-1}$	energy	τ (ps)	energy	expt.[16]
0^0	20776.6	344.0		20403.7	302	20403.7	
0^0_g(I)	208.8	0.484					
6^1	283.2	0.385	283.2	192.6	1.137		
0^0_u(I)	183.9	0.677					
6^2	454.1	0.229	170.9	451.0	0.104	478/493[a]	450 ± 30
6^3	609.4	0.109	155.3	618.9	0.061		
6^4	787.9	0.0674	178.4				
6^5	1013.7	0.0471	225.8.				
4^1	703.9	18.0					
$4^1 6^2$	1107.4	0.177					
3^1	1166.0	8.75	1166.0	1124.6	1.087	1126/1121[a]	1165 ± 10
$3^1 6^1$	1374.6	0.233					
$3^1 6^3$	1684.2	0.0492					
$3^1 4^1$	1847.6	0.701					
3^2	2322.6	2.52	1156.6	2238.2	0.280		2330 ± 30
$3^2 4^1$	2984.5	0.582					
3^3	3465.0	1.37	1142.3				
2^1	1659.6	24.5		1645.4	16.85	1646	1635 ± 10
$2^1 6^1$	1897.1	2.72					
$2^1 6^3$	2007.3	0.346					
$2^1 4^1$	2363.7	28.5					
$2^1 3^1$	2822.0	10.4		2766.5	1.390	2769/2766[a]	2800 ± 30
$2^1 3^1 4^1$	3505.3	6.08					
$2^1 3^2$	3972.3	3.44					
$2^2 6^1$	3572.2	3.62					
$2^2 4^1$	4006.4	6.75					

[a]Energies of the tunneling doublet.

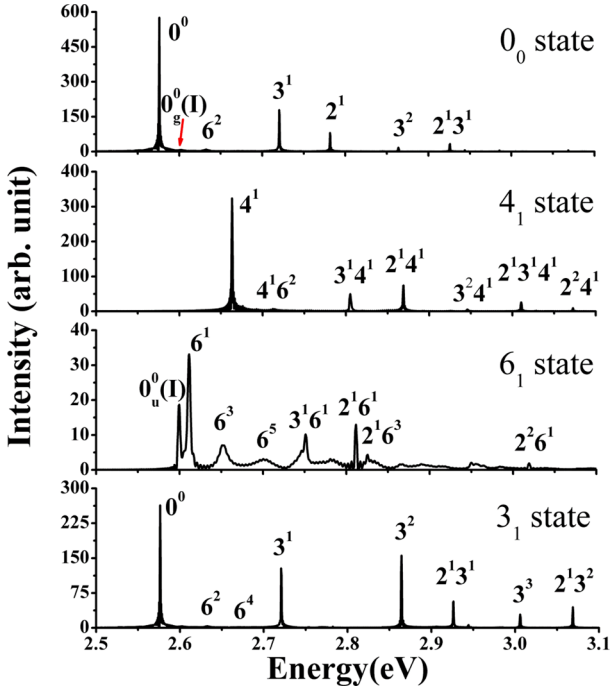

Figure 6. Photoelectron spectra for the 0_0, 4_1 (759.4 cm^{-1}), 6_1 (853.6 cm^{-1}), and 3_1 (1297.2 cm^{-1}) states of the H_2CC^- anion.

the absorbed peaks are listed in Table 3. The spectrum from the ground vibrational state of the anion is dominated by a strong peak for the 0^0_0 transition. This is due to the fact that the equilibrium geometries of both the neutral and anionic vinylidene species are quite close, as shown in Table 1. From this feature, we determined the adiabatic electron affinity (AEA) to be 0.477 eV, close to the experimental one of 0.490 eV.[16] The other peaks include the 3^1_0, 3^2_0, 2^1_0, and $2^1_0 3^1_0$ features, reflecting the small but noticeable geometric differences in the θ_{HCC} and r_{CC} coordinates.

The spectrum for the 4_1 state has a similar structure as those for the ground vibrational state. It is dominated by the 4^1_1 transition, and the transitions of $3^1_0 4^1_1$, $2^1_0 4^1_1$, and $2^1_0 3^1_0 4^1_1$ have weaker intensities. The 0^0_0 and 4^1_1 features, at 0.477 and 0.483 eV, are very close in energy, but the latter contributes ten times less than the former in the thermal spectrum, due to its small Boltzmann factor at 450 K. As a result, the 4^1_1 transition does not manifest as a distinct feature in a low-resolution thermal spectrum shown in Figure 5.

The spectrum for the 6_1 state of the anion is quite different from the 0_0 and 4_1 ones discussed above. Although it is dominated by the 6^1_1 transition, there are quite a few interesting features. First, comparing with the 0_0 and 4_1 spectra, most peaks in the 6_1 spectrum have large spectral widths, which indicate that the lifetimes of the vibrational states in the ν_6 progression are much shorter than other modes. This is due to the fact that the CH_2 rocking mode has a larger projection on the isomerization reaction coordinate for the vinylidene-acetylene isomerization. Second, the energy difference of $6^3_1 - 6^1_1 = 326$ cm^{-1} is much smaller than $6^5_1 - 6^3_1 = 404$ cm^{-1} due to anharmonicity. Third, there is an auxiliary peak denoted as 0^0_u(I), which has stronger intensity in the spectrum than the 6^3_1 feature. These two latter features are due to the triple-well feature on the PES, as shown in Figure 1. Specifically, the INT wells not only perturb the energy of adjacent levels but also

DOI: 10.1021/acs.jpca.5b05061
J. Phys. Chem. A 2015, 119, 8488−8496

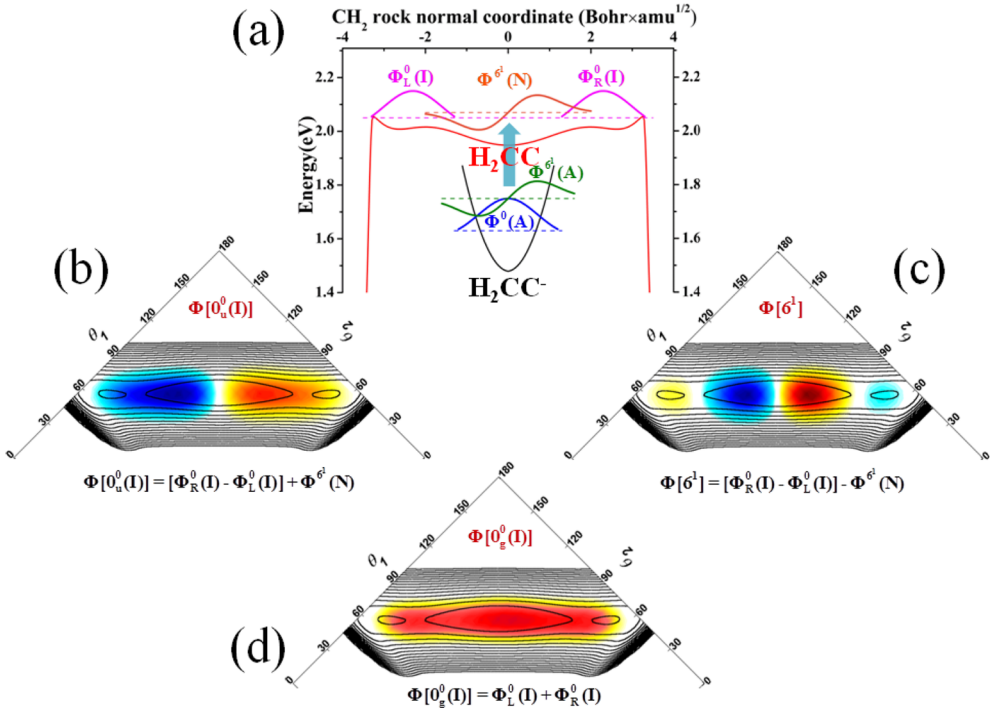

Figure 7. Scheme for the formation mechanism of the states of $0_g^0(I)$, $0_u^0(I)$, and 6^1 in the photoelectron spectra. (a) The MEPs of the H_2CC^- anion and H_2CC are expressed in mass-weighted Cartesian coordinates of the CH_2 rock mode of H_2CC species. The schematic diagrams of uncoupled low-lying vibrational states of the H_2CC^- anion and H_2CC are expressed at the corresponding locations in the MEPs, where $\Phi_L^0(I)$ and $\Phi_R^0(I)$ are the "left" and "right" ground states in the INT wells, where "I" denotes the wave functions locate at the INT minima. $\Phi^{6^1}(N)$ and $\Phi^{6^1}(A)$ are the first excited state of the CH_2 rocking mode for neutral and anionic vinylidene, while $\Phi^0(A)$ denotes the ground state of the anion. (b–d) The wave functions of the $0_u^0(I)$, 6^1, and $0_g^0(I)$ states are shown in Radau coordinates with the two-dimensional minimum energy surface.

involve indirect coupling of nearby states of vinylidene. These states are denoted as $0_g^0(I)$ and $0_u^0(I)$ in Table 3 (I for INT). In Figure 7a, the MEPs of the H_2CC^- anion and the H_2CC are expressed in mass-weighted Cartesian coordinates of the CH_2 rocking mode of the H_2CC species. The two identical INT wells accommodate two degenerate local states, which can be labeled as $\Phi_L^0(I)$ and $\Phi_R^0(I)$. Their linear combinations, $\Phi_L^0(I)+\Phi_R^0(I)$ and $\Phi_L^0(I)-\Phi_R^0(I)$, lead to two near-degenerate states, which have even and odd symmetries. Because of its odd symmetry, the first excited CH_2 rocking mode, $\Phi^{6^1}(N)$, only couples with the $\Phi_L^0(I)-\Phi_R^0(I)$ state, forming the $0_u^0(I)$ (Figure 7b) and 6^1 (Figure 7c) states, with the former at a lower energy. To the best of our knowledge, this is the first time that large amplitude vibrational states that are of neither the acetylene nor vinylidene character have been identified. The strong $0_u^0(I)$ peak directly related to the INT wells can be taken as evidence for the existence of INT states. On the other hand, the $0_g^0(I)$ state (Figure 7d) has a different symmetry and is thus not involved in the transition.

The spectrum from the 3_1 state is dominated by the 3_1^{0-2} transitions, and there are three weaker peaks ($2_0^1 3_1^1$, 3_1^3, and $2_0^1 3_1^2$). Additionally, two short-lived peaks of $3_1^0 6_0^2$ and $3_1^0 6_0^4$ are observed with very small intensities. All of the strong peaks in the 3_1 spectrum are long-lived, as shown in Table 3.

The positions and lifetimes of the vinylidene peaks are collected in Table 3, along with the available experimental data and values reported by previous theoretical studies. Note in particular that the lifetime for the ground vibrational state of vinylidene is exceedingly long, reflecting presumably the tunneling nature of this state. On the other hand, the lifetimes of 6^n states are short, consistent with the pivotal role of the CH_2 rocking mode in the isomerization reaction coordinate. Overall, the calculated energy levels in the present work are in good agreement with the experiment.[16] The agreement with the previous theoretical values reported by Bian and co-workers[55,56] using the ZB PES is also reasonable. As shown in the table, however, their energies, particularly for the 6^n states, are significantly different from our results and the experimental values. Significant differences also exist among the values from the same group. We conclude that our new PES represents a substantial improvement over the ZB PES in both the acetylene and vinylidene regions. As discussed in our previous work,[58] the errors in the ZB PES are most likely due to those introduced in the fitting process, rather than the level of the ab initio calculations. We also note that the existence of the INT minima seems to have a significant effect on the vinylidene states.

As mentioned in Section III, the "lifetimes" of the vinylidene states are computed here in the limit of an infinite density of states for acetylene. While the acetylene density of states is indeed very high near the isomerization barrier, it is for sure not infinity. In addition, not all acetylene vibrational states will interact effectively with the vinylidene ones. Most likely, the isomerization will be promoted by acetylene local bending modes and by vinylidene CH_2 rocking modes, and the former has a substantially lower density of states. It has been estimated that under the photodetachment experimental conditions there are only a few such states at the relevant energy range.[13] As a result, the lifetimes reported in Table 3 can only be regarded as a lower bound, which corresponds to the low-resolution spectrum. Indeed, Lineberger and co-workers have explicitly stated that the vinylidene widths only provide a lower bound to lifetimes.[16] Furthermore, because the interaction will not only

DOI: 10.1021/acs.jpca.5b05061
J. Phys. Chem. A 2015, 119, 8488–8496

depend on the coupling strengths between the two but also their energy differences, the accidental nature of the latter might result in large vibrational level shifts and widely irregular "lifetimes" or even quantum beating. These possible spectroscopic signatures can indeed be probed experimentally.

Rigorously speaking, the lifetime for bound states of both acetylene and vinylidene are infinity. However, it is possible to define the time scale for intramolecular vibrational energy redistribution (IVR),[78] which describes the rate of energy flow between the vinylidene and acetylene vibrational modes. The IVR rate depends on a number of factors, including the density of states, anharmonic resonances, and Coriolis coupling, etc. From this IVR perspective, the results of the photodetachment[16] and Coulomb explosion experiments[17] can be reconciled: the former measured the short-time dynamics of the vinylidene wave packet prepared by photodetachment, while the latter probed the long time behavior of the same species. In other words, the former is related to the initial decay of the autocorrelation function, while the latter its long-time recurrence. The calculations reported here pertains more closely to the former, and the latter is beyond the current model as it requires an adequate treatment of both the vinylidene and acetylene vibrations.

V. CONCLUSIONS

In this work, we report a full-dimensional quantum study of the early dynamics of vinylidene prepared by photodetaching the corresponding anion. The calculations were carried out using an exact kinetic energy operator and accurate ab initio based PESs for both the anionic and neutral species. The anion PES reported in this work is accurate, as evidenced by the reproduction of the known experimental vibrational frequencies. The neutral PES, which has been demonstrated to be accurate in describing the acetylene vibration in our earlier work,[58] is also shown to be of near-spectroscopic accuracy in the vinylidene region. Both positions and "lifetimes" of the vinylidene vibrational features have been obtained, the latter in the limit of an infinite density of states. The agreement with experimental energies is much better than previous theoretical studies, underscoring the much improved accuracy of the new PES.

The global PES will be instrumental in studying the acetylene−vinylidene isomerization dynamics in the future. As pointed out recently by Prozument et al.,[13] a particular interesting scenario is the dynamics of rotationally excited vinylidene, where the Coriolis coupling will allow very effective coupling with local benders of acetylene. It has been shown that the IVR is quite fast for local benders with sufficient rotational excitation,[79] which might render the isomerization of vinylidene approaching the infinite density of states limit. This is probably the reason why no vinylidene was observed in the latest experiment with the Chirped Pulse millimeter Wave (CPmmW) method.[13] To understand the role of the Coriolis coupling theoretically, $J > 0$ calculations of vibrational states have to be performed in both acetylene and vinylidene wells on an accurate global PES. The interplay between experimental and theoretical studies will ultimately provide a comprehensive understanding of this prototypical system.

AUTHOR INFORMATION

Corresponding Authors

*E-mail: majianyi81@163.com. Tel: +86 028 85405515.
*E-mail: hguo@unm.edu. Tel: 505 2771716.

Notes

The authors declare no competing financial interest.

ACKNOWLEDGMENTS

J.M. acknowledges the National Natural Science Foundation of China (Grant 21303110) for support. The work at UNM was supported by the U.S. Department of Energy (DF-FG02-05ER15694 to H.G.). H.G. thanks Bob Field for many stimulating discussions. Part of the calculations were carried out at the National Energy Research Scientific Computing (NERSC) Center.

REFERENCES

(1) Duran, R. P.; Amorebieta, V. T.; Colussi, A. J. Pyrolysis of Acetylene: A Thermal Source of Vinylidene. *J. Am. Chem. Soc.* **1987**, *109*, 3154−3155.
(2) Schaefer, H. F., III The 1,2 Hydrogen Shift: A Common Vehicle for the Disappearance of Evanescent Molecular Species. *Acc. Chem. Res.* **1979**, *12*, 288−296.
(3) Lundberg, J. K., The SEP Spectrum of Acetylene: Symmetry Properties and Isomerization. In *Molecular Dynamics and Spectroscopy*, Dai, H. L., Field, R. W., Eds. World Scientific: Singapore, 1995.
(4) Herman, M.; Lievin, J.; VanderAuwera, J.; Campargue, A. Global and Accurate Vibration Hamiltonians from High Resolution Molecular Spectroscopy. *Adv. Chem. Phys.* **1999**, *108*, 1−431.
(5) Jacobson, M. P.; Field, R. W. Acetylene at the Threshold of Isomerization. *J. Phys. Chem. A* **2000**, *104*, 3073−3086.
(6) Kellman, M. E.; Tyng, V. The Dance of Molecules: New Dynamical Perspectives on Highly Excited Molecular Vibrations. *Acc. Chem. Res.* **2007**, *40*, 243−250.
(7) Chen, Y.; Jonas, D. M.; Kinsey, J. L.; Field, R. W. High Resolution Spectroscopic Detection of Acetylene-Vinylidene Isomerization by Spectral Cross Correlation. *J. Chem. Phys.* **1989**, *91*, 3976−3987.
(8) Yamanouchi, K.; Ikeda, N.; Tsuchiya, S.; Jonas, D. M.; Lundberg, J. K.; Adamson, G. W.; Field, R. W. Vibrational Highly Excited Acetylene as Studied by Dispersed Fluorescence and Stimulated Emission Pumping Spectroscopy: Vibrational Assignment of the Feature States. *J. Chem. Phys.* **1991**, *95*, 6330−6342.
(9) Jonas, D. M.; Solina, S. A. B.; Rajaram, B.; Silbey, R. J.; Field, R. W.; Yamanouchi, K.; Tschiya, S. Intramolecular Vibrational Redistribution of Energy in the Stimulated Emission Pumping Spectrum of Acetylene. *J. Chem. Phys.* **1993**, *99*, 7350−7370.
(10) Solina, S. A. B.; O'Brien, J. P.; Field, R. W.; Polik, W. F. Dispersed Fluorescence Spectrum of Acetylene from the A^1A_u Origin: Recognition of Polyads and Test of Multiresonance Effective Hamiltonian Model for the X State. *J. Phys. Chem.* **1996**, *100*, 7797−7809.
(11) O'Brien, J. P.; Jacobson, M. P.; Sokol, J. J.; Coy, S. L.; Field, R. W. Numerical Pattern Recognition Analysis of Acetylene Dispersed Fluorescence Spectra. *J. Chem. Phys.* **1998**, *108*, 7100.
(12) Jacobson, M. P.; O'Brien, J. P.; Field, R. W. Anomalously Slow Intramolecular Vibrational Redistribution in the Acetylene X State above 10000 cm^{-1} of Internal Energy. *J. Chem. Phys.* **1998**, *109*, 3831−3840.
(13) Prozument, K.; Shaver, R. G.; Ciuba, M. A.; Muenter, J. S.; Park, G. B.; Stanton, J. F.; Guo, H.; Wong, B. M.; Perry, D. S.; Field, R. W. A New Approach toward Transition State Spectroscopy. *Faraday Discuss.* **2013**, *163*, 33−57.
(14) Jacobson, M. P.; Silbey, R. J.; Field, R. W. Local Mode Behavior in the Acetylene Bending System. *J. Chem. Phys.* **1999**, *110*, 845−859.
(15) Burnett, S. M.; Stevens, A. E.; Feigerle, C. S.; Lineberger, W. C. Observation of X^1A_1 Vinylidene by Photoelectron Spectroscopy of the $C_2H_2^-$ Ion. *Chem. Phys. Lett.* **1983**, *100*, 124−128.
(16) Ervin, K. M.; Ho, J.; Lineberger, W. C. A Study of the Singlet and Triplet States of Vinylidene by Photoelectron Spectroscopy of $H_2C{=}C^-$, $D_2C{=}C^-$, and $HDC{=}C^-$. Vinylidene-Acetylene Isomerization. *J. Chem. Phys.* **1989**, *91*, 5974−5992.

DOI: 10.1021/acs.jpca.5b05061
J. Phys. Chem. A 2015, 119, 8488−8496

(17) Levin, J.; Feldman, H.; Baer, A.; Ben-Hamu, D.; Heber, O.; Zajfman, D.; Vager, Z. Study of Unimolecular Reactions by Coulomb Explosion Imaging: The Nondecaying Vinylidene. *Phys. Rev. Lett.* **1998**, *81*, 3347−3350.
(18) Kellman, M. E.; Chen, G. Approximate Constants of Motion and Energy Transfer Pathways in Highly Excited Acetylene. *J. Chem. Phys.* **1991**, *95*, 8671−8672.
(19) Rose, J. P.; Kellman, M. E. Bending Dynamics from Acetylene Spectra: Normal, Local, and Precessional Modes. *J. Chem. Phys.* **1996**, *105*, 10743−10754.
(20) Sibert, E. L.; McCoy, A. B. Quantum, Semiclassical and Classical Dynamics of the Bending Modes of Acetylene. *J. Chem. Phys.* **1996**, *105*, 469−478.
(21) McCoy, A. B.; Sibert, E. L. The Bending Dynamics of Acetylene. *J. Chem. Phys.* **1996**, *105*, 459.
(22) Jacobson, M. P.; O'Brien, J. P.; Silbey, R. J.; Field, R. W. Pure Bending Dynamics in the Acetylene X State up to 15000 cm^{-1} of Internal Energy. *J. Chem. Phys.* **1998**, *109*, 121−133.
(23) Jacobson, M. P.; Jung, C.; Taylor, H. S.; Field, R. W. State-by-State Assignment of the Bending Spectrum of Acetylene at 15000 cm^{-1}: A Case Study of Quantum-Classical Correspondence. *J. Chem. Phys.* **1999**, *111*, 600−618.
(24) Prosmiti, R.; Farantos, S. C. Periodic Orbits and Bifurcation Diagrams of Acetylene/Vinylidene Revisited. *J. Chem. Phys.* **2003**, *118*, 8275−8280.
(25) Tyng, V.; Kellman, M. E. Bending Dynamics of Acetylene: New Modes Born in Bifurcations of Normal Modes. *J. Phys. Chem. B* **2006**, *110*, 18859.
(26) Tyng, V.; Kellman, M. E. Catastrophe Map and the Role of Individual Resonances in C_2H_2 Bending Dynamics. *J. Chem. Phys.* **2009**, *130*, 144311.
(27) Tyng, V.; Kellman, M. E. Critical Points Bifurcation Analysis of High-*J* Bending Dynamics in Acetylene. *J. Chem. Phys.* **2009**, *131*, 244111.
(28) Park, G. B.; Baraban, J. H.; Field, R. W. Full Dimensional Franck-Condon Factors for the Acetylene $\tilde{A}^1A_u$—$\tilde{X}^1\Sigma_g^+$ Transition. II. Vibrational Overlap Factors for Levels Involving Excitation in Ungerade Modes. *J. Chem. Phys.* **2014**, *141*, 134305.
(29) Xu, D.; Li, G.; Xie, D.; Guo, H. Full-Dimensional Quantum Calculations of Vibrational Energy Levels of Acetylene (HCCH) up to 13000 cm^{-1}. *Chem. Phys. Lett.* **2002**, *365*, 480−486.
(30) Xu, D.; Chen, R.; Guo, H. Probing Highly Excited Vibrational Eigenfunctions Using a Modified Single Lanczos Method: Application to Acetylene (HCCH). *J. Chem. Phys.* **2003**, *118*, 7273−7282.
(31) Ma, J.; Xu, D.; Guo, H.; Tyng, V.; Kellman, M. E. Isotope Effect in Normal-to-Local Transition of Acetylene Bending Modes. *J. Chem. Phys.* **2012**, *136*, 014304.
(32) Zhang, Z.; Li, B.; Shen, Z.; Ren, Y.; Bian, W. Efficient Quantum Calculation of the Vibrational States of Acetylene. *Chem. Phys.* **2012**, *400*, 1−7.
(33) Carrington, T., Jr.; Hubbard, L. M.; Schaefer, H. F.; Miller, W. H. Vinylidene: Potential Energy Surface and Unimolecular Reaction Dynamics. *J. Chem. Phys.* **1984**, *80*, 4347−4354.
(34) Germann, T. C.; Miller, W. H. Quantum Mechanical Calculation of Resonance Tunneling in Acetylene Isomerization via the Vinylidene Intermediate. *J. Chem. Phys.* **1998**, *109*, 94−101.
(35) Schork, R.; Koppel, H. *ab initio* Quantum Dynamical Study of the Vinylidene-Acetylene Isomerization. *Theor. Chem. Acc.* **1998**, *100*, 204−211.
(36) Hayes, R. L.; Fattal, E.; Govind, N.; Carter, E. A.; Long Live. Vinylidene! A New View of the $H_2CC \rightarrow HCCH$ Rearrangement from *ab initio* Molecular Dynamics. *J. Am. Chem. Soc.* **2001**, *123*, 641−657.
(37) Schork, R.; Koppel, H. Barrier Recrossing in the Vinylidene-Acetylene Isomerization Reaction: A Five-Dimensional *ab initio* Quantum Dynamical Investigation. *J. Chem. Phys.* **2001**, *115*, 7907.
(38) Zou, S.; Bowman, J. M. Reduced Dimensionality Quantum Calculations of Acetylene-Vinylidene Isomerization. *J. Chem. Phys.* **2002**, *116*, 6667−6673.
(39) Wong, B. M.; Thom, R. L.; Field, R. W. Accurate Inertias for Large-Amplitude Motions: Improvements on Prevailing Approximations. *J. Phys. Chem. A* **2006**, *110*, 7406−7413.
(40) Carter, S.; Mills, I. M.; Murrell, J. N. A Potential Energy Surface for the Ground State of Acetylene, $H_2C_2(X^1\Sigma_g^+)$. *Mol. Phys.* **1980**, *41*, 191−203.
(41) Halonen, L.; Child, M. S.; Carter, S. Potential Models and Local Mode Vibrational Eigenvalue Calculations for Acetylene. *Mol. Phys.* **1982**, *47*, 1097−1112.
(42) Bramley, M. J.; Carter, S.; Handy, N. C.; Mills, I. M. A Refined Quartic Forcefield for Acetylene: Accurate Calculations of the Vibrational Spectrum. *J. Mol. Spectrosc.* **1993**, *157*, 301−336.
(43) Chang, N.-y.; Shen, M.-y.; Yu, C.-h. Extended *ab initio* Studies of the Vinylidene−Acetylene Rearrangement. *J. Chem. Phys.* **1997**, *106*, 3237−3242.
(44) Stanton, J. F.; Gauss, J. An Estimation of the Isomerization Energy of Acetylene. *J. Chem. Phys.* **1999**, *110*, 1831−1832.
(45) Stanton, J. F.; Gauss, J. Vibrational Structure in the Vinylidene Anion Photoelectron Spectrum: Closing the Gap between Theory and Experiment. *J. Chem. Phys.* **1999**, *110*, 6079−6080.
(46) Joseph, S.; Varandas, A. J. C. Accurate MRCI and CC Study of the Most Relevant Stationary Points and Other Topographical Attributes for the Ground-State C_2H_2 Potential Energy Surface. *J. Phys. Chem. A* **2010**, *114*, 13277−13287.
(47) Lee, H.; Baraban, J. H.; Field, R. W.; Stanton, J. F. High-Accuracy Estimates for the Vinylidene-Acetylene Isomerization Energy and the Ground State Rotational Constants of $:C{=}CH_2$. *J. Phys. Chem. A* **2013**, *117*, 11679−11683.
(48) Zou, S.; Bowman, J. M. A New *ab initio* Potential Energy Surface Describing the Acetylene/Vinylidene Isomerization. *Chem. Phys. Lett.* **2003**, *386*, 421−424.
(49) Zou, S.; Bowman, J. M.; Brown, A. Full Dimensionality Quantum Calculations of Acetylene/Vinylidene Isomerization. *J. Chem. Phys.* **2003**, *118*, 10012−10023.
(50) Kozin, I. N.; Law, M. M.; Tennyson, J.; Hutson, J. M. Calculating Energy Levels of Isomerizing Tetra-Atomic Molecules: II. The Vibrational States of Acetylene and Vinylidene. *J. Chem. Phys.* **2005**, *122*, 064309.
(51) Zou, S.; Bowman, J. M. Full Dimensionality Quantum Calculations of Acetylene/Vinylidene Isomerization. *J. Chem. Phys.* **2002**, *117*, 5507−5511.
(52) Tremblay, J. C.; Carrington, T., Jr. Calculating Vibrational Energies and Wave Functions of Vinylidene Using a Contracted Basis with a Locally Reorthogonalized Coupled Two-Term Lanczos Eigensolver. *J. Chem. Phys.* **2006**, *125*, 094311.
(53) Li, B.; Bian, W. Efficient Quantum Calculations of Vibrational States of Vinylidene in Full Dimensionality: A Scheme with Combination of Methods. *J. Chem. Phys.* **2008**, *129*, 024111.
(54) Ren, Y.; Li, B.; Bian, W. Full-Dimensional Quantum Dynamics Study of Vinylidene-Acetylene Isomerization: A Scheme Using the Normal Mode Hamiltonian. *Phys. Chem. Chem. Phys.* **2011**, *13*, 2052−2061.
(55) Li, B.; Ren, Y.; Bian, W. Accurate Quantum Dynamics Study on the Resonance Decay of Vinylidene. *ChemPhysChem* **2011**, *12*, 2419−2422.
(56) Ren, Y.; Bian, W. Mode-Specific Tunneling Splittings for a Sequential Double-Hydrogen Transfer Case: An Accurate Quantum Mechanical Scheme. *J. Phys. Chem. Lett.* **2015**, 1824−1829.
(57) Xu, D.; Guo, H.; Zou, S.; Bowman, J. M. A Scaled *ab initio* Potential Energy Surface for Acetylene and Vinylidene. *Chem. Phys. Lett.* **2003**, *377*, 582−588.
(58) Han, H.; Li, A.; Guo, H. Towards Spectroscopically Accurate Global *ab initio* Potential Energy Surface for the Acetylene-Vinylidene Isomerization. *J. Chem. Phys.* **2014**, *141*, 244312.
(59) Jiang, B.; Guo, H. Permutation Invariant Polynomial Neural Network Approach to Fitting Potential Energy Surfaces. *J. Chem. Phys.* **2013**, *139*, 054112.

DOI: 10.1021/acs.jpca.5b05061
J. Phys. Chem. A 2015, 119, 8488−8496

(60) Li, J.; Jiang, B.; Guo, H. Permutation Invariant Polynomial Neural Network Approach to Fitting Potential Energy Surfaces. II. Four-Atomic Systems. *J. Chem. Phys.* **2013**, *139*, 204103.
(61) Adler, T. B.; Knizia, G.; Werner, H.-J. A Simple and Efficient CCSD(T)-F12 Approximation. *J. Chem. Phys.* **2007**, *127*, 221106.
(62) Knizia, G.; Adler, T. B.; Werner, H.-J. Simplified CCSD(T)-F12 Methods: Theory and Benchmarks. *J. Chem. Phys.* **2009**, *130*, 054104.
(63) Peterson, K. A.; Adler, T. B.; Werner, H.-J. Systematically Convergent Basis Sets for Explicitly Correlated Wavefunctions: The Atoms H, He, B−Ne, and Al−Ar. *J. Chem. Phys.* **2008**, *128*, 084102.
(64) Hill, J. G.; Mazumder, S.; Peterson, K. A. Correlation Consistent Basis Sets for Molecular Core-Valence Effects with Explicitly Correlated Wave Functions: The Atoms B−Ne and Al−Ar. *J. Chem. Phys.* **2010**, *132*, 054108.
(65) Gerardi, H. K.; Breen, K. J.; Guasco, T. L.; Weddle, G. H.; Gardenier, G. H.; Laaser, J. E.; Johnson, M. A. Survey of Ar-Tagged Predissociation and Vibrationally Mediated Photodetachment Spectroscopies of the Vinylidene Anion, $C_2H_2^-$. *J. Phys. Chem. A* **2010**, *114*, 1592−1601.
(66) Werner, H. J.; Knowles, P. J.; Knizia, G.; Manby, F. R.; Schütz, M. Molpro: A General-Purpose Quantum Chemistry Program Package. *Wiley Interdiscip. Rev.: Comput. Mol. Sci.* **2012**, *2*, 242−253.
(67) Xie, Z.; Bowman, J. M. Permutationally Invariant Polynomial Basis for Molecular Energy Surface Fitting Via Monomial Symmetrization. *J. Chem. Theor. Comp.* **2010**, *6*, 26−34.
(68) Yu, H.-G.; Muckerman, J. T. A General Variational Algorithm to Calculate Vibrational Energy Levels of Tetraatomic Molecules. *J. Mol. Spectrosc.* **2002**, *214*, 11−20.
(69) Chen, R.; Ma, G.; Guo, H. Six-Dimensional Quantum Calculation of Highly Excited Vibrational Energy Levels of Hydrogen Peroxide and Its Deuterated Isotopomers. *J. Chem. Phys.* **2001**, *114*, 4763−4774.
(70) Light, J. C.; Carrington, T., Jr. Discrete-Variable Representations and Their Utilization. *Adv. Chem. Phys.* **2000**, *114*, 263−310.
(71) Echave, J.; Clary, D. C. Potential Optimized Discrete Variable Representation. *Chem. Phys. Lett.* **1992**, *190*, 225−230.
(72) Wei, H.; Carrington, T., Jr. The Discrete Variable Representation of a Triatomic Hamiltonian in Bond Length Bond Angle Coordinates. *J. Chem. Phys.* **1992**, *97*, 3029−3037.
(73) Ma, J.; Guo, H. Full-Dimensional Quantum State Resolved Predissociation Dynamics of HCO_2 Prepared by Photodetaching HCO_2^-. *Chem. Phys. Lett.* **2011**, *511*, 193−195.
(74) Otto, R.; Ma, J.; Ray, A. W.; Daluz, J. S.; Li, J.; Guo, H.; Continetti, R. E. Imaging Dynamics on the F + H_2O → HF + OH Potential Energy Surfaces from Wells to Barriers. *Science* **2014**, *343*, 396−399.
(75) Guo, H. Recursive Solutions to Large Eigenproblems in Molecular Spectroscopy and Reaction Dynamics. *Rev. Comput. Chem.* **2007**, *25*, 285−347.
(76) Chen, R.; Guo, H. The Chebyshev Propagator for Quantum Systems. *Comput. Phys. Commun.* **1999**, *119*, 19−31.
(77) Guo, H. A Time-Independent Theory of Photodissociation Based on Polynomial Propagation. *J. Chem. Phys.* **1998**, *108*, 2466−2472.
(78) Nesbitt, D. J.; Field, R. W. Vibrational Energy Flow in Highly Excited Molecules: Role of Intramolecular Vibrational Redistribution. *J. Phys. Chem.* **1996**, *100*, 12735−12756.
(79) Perry, D. S.; Martens, J.; Amyay, B.; Herman, M. Hierarchies of Intramolecular Vibration−Rotation Dynamical Processes in Acetylene up to 13,000 cm^{-1}. *Mol. Phys.* **2012**, *110*, 2687−2705.

DOI: 10.1021/acs.jpca.5b05061
J. Phys. Chem. A 2015, 119, 8488−8496